Optical emission from C_{60}-coupled β-$FeSi_2$ nanocomposites

X. L. Wu,[a] F. S. Xue, and Z. Y. Zhang
National Laboratory of Solid State Microstructures, Nanjing University, Nanjing 210093, People's Republic of China

Paul K. Chu
Department of Physics and Materials Science, City University of Hong Kong, Kowloon, Hong Kong, People's Republic of China

(Received 19 July 2006; accepted 26 October 2006; published online 7 December 2006)

C_{60}-coupled β-$FeSi_2$ nanocomposite structures were fabricated and their photoluminescence (PL) properties were investigated. The nanocomposites exhibit a pinned PL peak at 570 nm and a band edge at ~370 nm. Spectral analyses suggest that the pinned PL behavior is closely related to both the β-$FeSi_2$ nanocrystals and the coupled C_{60}. A band-mixing model based on the direct and indirect gaps in a nanoenvironment consisting of mainly β-$FeSi_2$ nanocrystals and C_{60} is proposed and used to derive the electronic states. Good agreement is achieved between the theoretical calculation and experimental results. © *2006 American Institute of Physics*. [DOI: 10.1063/1.2402892]

The electronic states and photoluminescence (PL) properties of nanocomposites (NCs) have attracted considerable attention in recent years because of potential applications in optoelectronics.[1–7] Previous studies have indicated that the PL behavior of a NC cannot be explained simply by a single mechanism such as quantum confinement,[1] surface states,[3,4,8] or defect centers.[9] This also applies to the simplest NC consisting of a core and its shell layer, as the PL behavior is a result of the interaction between the electronic states of the core and shell layer.[2–7] A typical example is the Fe-passivated porous Si ($Si/FeSi_2$) presented by Zhang *et al.*[10] When stored in air, the $Si/FeSi_2$ NC shows the PL intensity enhancement, but the peak position keeps unchanged. Recently, we explained the PL behavior based on the energy band-mixing model.[11] We found that unique direct (0.83 eV) (Refs. 12 and 13) and indirect (0.78 eV) (Refs. 14 and 15) gap characters of the $FeSi_2$ layer strongly affect the PL property of the Si core. This indicates that studies on the $FeSi_2$ NCs are of important theoretical and experimental values. On the other hand, C_{60} molecule has a highly symmetrical structure and unique physical and chemical properties.[16] When it was placed in certain environments, the PL intensity related to C_{60} can greatly be improved.[17,18] So the C_{60}/β-$FeSi_2$ NC can be expected to have new light-emitting features.

In this work, we first fabricate β-$FeSi_2$ nanocrystals using anodization of Fe^+-implanted Si wafers. After chemically coupling C_{60} molecules onto the surface of the β-$FeSi_2$ nanocrystals, the β-$FeSi_2/C_{60}$ NC displays a pinned PL behavior due to the quantum confined geometry and host/guest interaction. Using the band-mixing model,[6] the electronic states of the NC are calculated and good agreement between the theoretical and experimental results is obtained.

⟨100⟩-oriented *p*-type Si wafer with a resistivity of 1–5 Ω cm was implanted with 3×10^{17} cm^{-2} Fe ions at 120 keV. The implanted Si wafer was annealed in N_2 at 1100 °C for 60 min, followed by anodization in a solution of ethanol:HF=1:2 (99.7% C_2H_5OH: 40% HF) for 20 min to form a porous structure. The PL spectra of two typical porous structures (samples A and B) are shown in Figs. 1(a) and 1(b) (solid lines). The two samples exhibit PL peaks at 610 and 660 nm with linewidths of ~120 nm. After storage in air, the PL peak positions remain unchanged, but their intensities increase with storage time and become saturated after four months. The PL excitation (PLE) spectra are shown in Figs. 1(c) and 1(d) (solid lines). It can be seen that the PLE peak redshifts with increasing the monitored wavelengths, suggesting that the photoexcited carriers occur in the band with quantum confinement.[19,20] Figure 2(a) depicts the Raman spectra acquired from samples A and B, from which we can infer that the two samples have mean Si nanocrystal

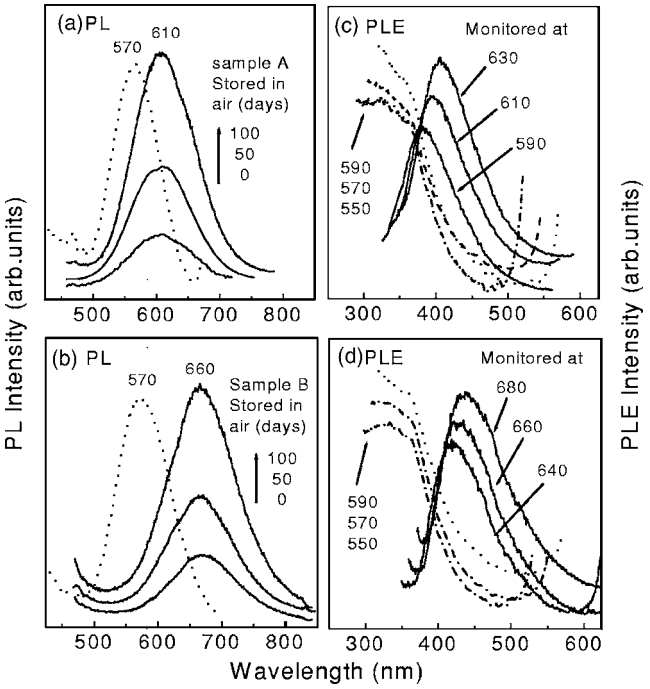

FIG. 1. PL spectra of (a) sample A and (b) sample B before (solid lines) and after (dotted line) C_{60} coupling. The etching current densities of samples A and B are 30 and 10 mA/cm^2, respectively. The PLE spectra of (c) sample A and (d) sample B before (solid lines) and after (dotted line) C_{60} coupling are also shown. The monitoring wavelengths are indicated in the figures.

[a]Author to whom correspondence should be addressed; electronic mail: hkxlwu@nju.edu.cn

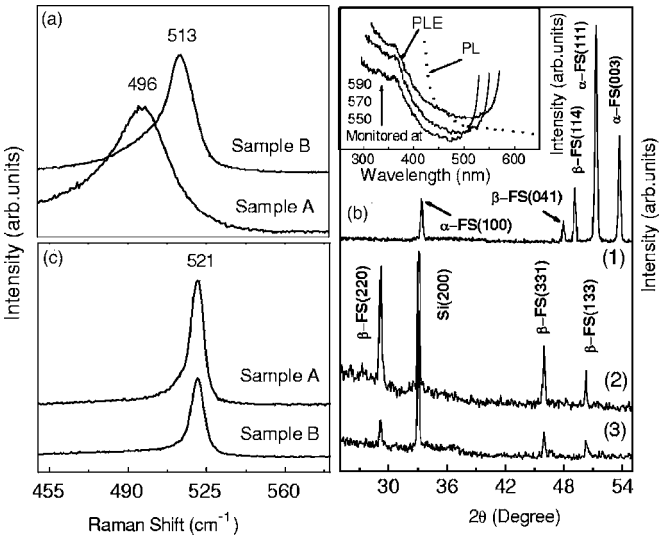

FIG. 2. Raman spectra acquired from samples A and B before (a) and after (c) C_{60} coupling. (b) XRD patterns of (1) Fe^+-implanted Si wafer annealed in N_2 at 1100 °C for 60 min and sample A before (2) and after (3) C_{60} coupling. The inset in (b) shows the PL and PLE spectra of sample A only coupled with the coupling agents.

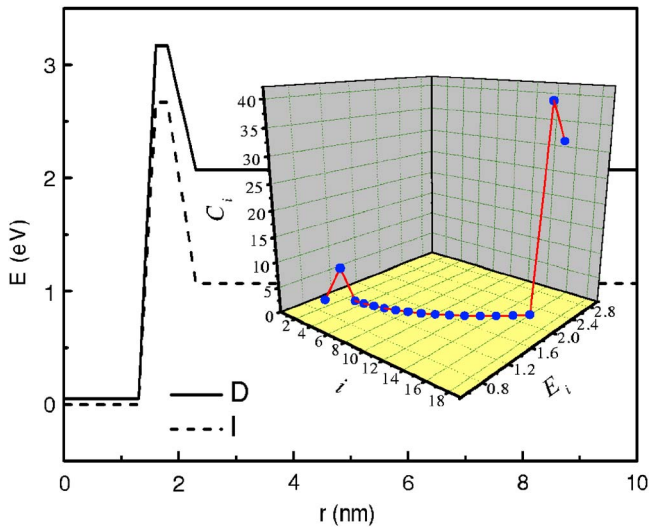

FIG. 4. (Color online) Band structure of the nanocomposite consisting of β-$FeSi_2$ core, (Ref. 14) the coupling agent layer with direct (3.17 eV) and indirect (2.67 eV) gaps, and the C_{60}-coupled layer with direct (2.07 eV) and indirect (1.07 eV) gaps (Ref. 28). We assume the effective masses of the indirect and direct gap states and hole to be $0.8m_0$ (Ref. 14). The solid and dashed lines illustrate the direct and indirect valleys in the conduction bands. The inset shows the calculated energy levels and their C coefficients.

sizes of 1.8 and 3.1 nm, respectively. It can thus be explained that the 610 and 660 nm PL peaks have an origin related to quantum confinement of the Si nanocrystals.[10,21] Curves (1) and (2) in Fig. 2(b) represent the x-ray diffraction (XRD) patterns of the annealed Fe^+-implanted Si wafer before and after anodization. Anodization destroys the original α-$FeSi_2$ nanocrystals while some new β-$FeSi_2$ nanocrystals are formed. Note that the XRD peak at ~33° has not changed its intensity in the anodizing sample. Thus, it is related to Si substrate.[22] Our high-resolution transmission electron microscopy (HRTEM) images also clearly show the existence of β-$FeSi_2$ nanocrystals with sizes of 1–5 nm (Fig. 3). The C_{60}-coupling experiments can be found elsewhere.[21,23] The presence of C_{60} in this coupling system was verified based on the Raman spectral analysis and atomic force microscopy images show that the coupled C_{60} clusters have sizes of ~20 nm.[24,25]

The dotted lines in Figs. 1(a) and 1(b) show the PL spectra of samples A and B with coupled C_{60}. The PL peaks are quite intense and pinned at 570 nm. Their linewidths are reduced to ~85 nm. The PL peak is very stable and no degradation can be observed after storage in air for more than three months. The dashed lines in Figs. 1(c) and 1(d) show the PLE spectra taken under three different monitoring wavelengths. All the PLE spectra are similar in shape and show the existence of a band edge at ~370 nm (3.35 eV). Figure 2(c) depicts the Raman spectra. Only the peak from the Si substrate at 521 cm^{-1} can be observed, indicating that Si nanocrystals have vanished after C_{60} coupling. However, it can be inferred from the XRD curve (3) of the C_{60}-coupled sample in Fig. 2(b) that C_{60} coupling process only decreases the β-$FeSi_2$ content. If we instead use a pure Si wafer to prepare similar C_{60}-coupled samples, no PL can be observed, suggesting that the pinned PL peak at 570 nm is closely related to the β-$FeSi_2$ nanocrystals. In addition, if we adopt steps 1 and 2 in the C_{60} coupling experiments to only combine the coupling agents with the β-$FeSi_2$ nanocrystals, the 570 nm PL peak cannot also be observed [the dotted line in the inset of Fig. 2(b)]. It implies that the 570 nm PL peak does not correlate with the coupling agent but depends on the coupled C_{60}. We have also found that the PLE spectra are very similar to those obtained from the C_{60}-coupled samples [the solid lines in the inset of Fig. 2(b)]. Thus, the pinned PL is closely related to the presence of both the β-$FeSi_2$ nanocrystals and coupled C_{60}. Such PL characteristics are evidently a result of the interaction between the C_{60} and β-$FeSi_2$ nanocrystals, and so we propose to use the band-mixing model to explain the origins of the pinned 570 nm PL and 370 nm PLE peaks.[6,26,27]

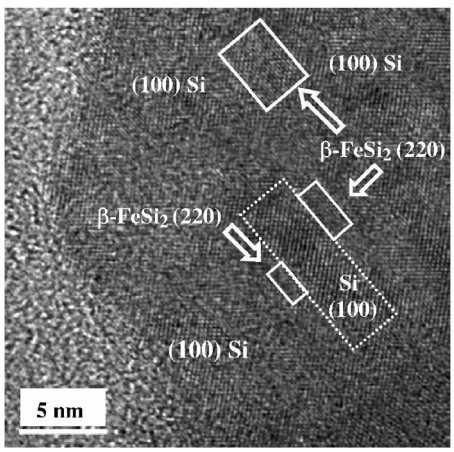

FIG. 3. Typical HRTEM image of the Fe^+-implanted Si wafer after anodization.

In our theoretical analysis, we consider the current β-$FeSi_2/C_{60}$ NC to consist of three nanolayers: a β-$FeSi_2$ core, a thin coupling agent layer (potential barrier), and an outer thick C_{60} layer with indirect gap.[28] The band-mixing model should be suitable for discussing the electronic structure of such size NCs.[7,11,15,27] The band structure of the NC is illustrated in Fig. 4 and the details of the band-mixing model can be found in Ref. 6. Here, we separate the wave function into direct and indirect gap waves. In each nanolayer, the lattice periodicity remains unchanged, so that the indirect and direct

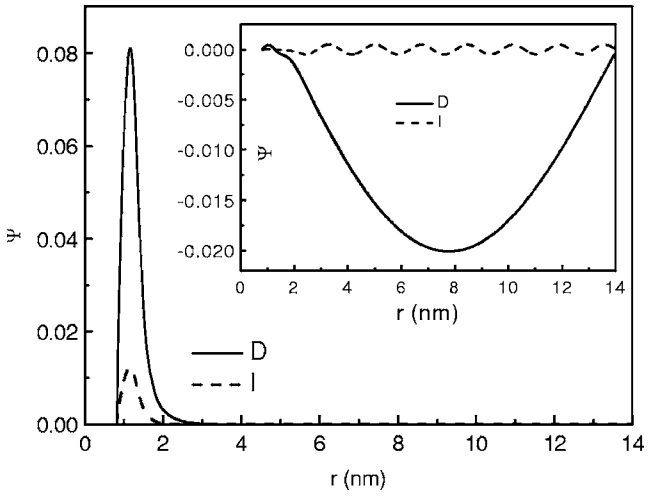

FIG. 5. Wave functions of the excited state E_2. The solid and dashed lines stand for the direct and indirect waves, respectively. The inset shows the wave functions of the excited state E_{17}. The Γ wave has extended into the coupling layer.

waves are independent and there is no coupling between the two waves. Owing to the broken lattice periodicity in the transition region between the two layers, the two waves will mix. Using the finite-difference method,[6,7] we can solve the Schrödinger equation in cylindrical coordinates to obtain the confined band-mixing energy levels. To effectively characterize the state attribution, a coupling coefficient $C=\bar{\Psi}_D/\bar{\Psi}_I$ is introduced, where Ψ_D and Ψ_I are the wave functions of the direct and indirect gap states, respectively. The inset of Fig. 4 shows the calculated energy levels and the C coefficients for different states. Since the width of the coupled C_{60} is rather large, most of the states are indirect gaps with weak emission (small C coefficient). Only the E_2 level with 1.14 eV has a large C_2 of 6.675 and shows a strong direct band. Its wave functions are shown in Fig. 5, in which the solid and dashed lines stand for the direct and indirect gap waves, respectively. We can see that both Ψ_D and Ψ_I are confined in the β-$FeSi_2$ quantum well due to the high barrier of the coupling agent. Because the hole effective mass in the β-$FeSi_2$ is equal to that of electron, $0.8m_0$, the calculated hole energy level is also larger, 0.276 eV. As a result, the transition energy ΔE_2 between the electron and hole levels, ΔE_2, is $1.14+0.276+0.78=2.196$ eV (565 nm) that is consistent with the energy of the pinned PL peak. With increasing energy levels, the confined states become indirect with low emission efficiency (small C) due to the confinement of the large-sized indirect C_{60} layer. This situation lasts up to the E_{16} level. The E_{17} level has an energy (2.228 eV) higher than that of the direct gap barrier of the coupled C_{60} layer, and so a new direct gap state appears and lasts at all times. The inset of Fig. 5 shows the wave functions of the lowest excitation state E_{17} with a large C coefficient. It can be seen that the wave functions have extended to the entire coupling layer. The transition energy ΔE_{17} between the electron and hole levels is $\Delta E_{17}=2.228+0.276+0.78=3.284$ eV (377 nm), which is the energy of the PLE peak. Since the energy levels higher than E_{17} all are direct, they constitute a continuous band like the absorption band in an indirect gap semiconductor caused by direct transition. This is again in agreement with our experimental PLE results.

We notice in our calculations that after coupling with the large-sized C_{60}, the PL and PLE peak energies hardly change because many lower energy levels induced by the confinement of the indirect C_{60} layer are all indirect states with low emission efficiencies. When the thickness of the coupling layer diminishes to half of the initial thickness, the indirect potential barrier is not sufficient to suppress the appearance of the direct gap excitation states. As a result, the PLE peak displays a large redshift. Furthermore, if the coupling layer is a direct gap material, the energies of the direct gap levels will be reduced due to the coupling. This should lead to more evident and we are currently conducting more experiments to corroborate our postulate.

This work was supported by Grant Nos. 10225416, 60576061, and BK2006715 from the National and JiangSu Natural Science Foundations and the LAPEM. Partial support was also from City University of Hong Kong Direct Allocation Grant No. 9360110.

[1] A. G. Cullis, L. T. Canham, and P. D. Calcott, J. Appl. Phys. **82**, 909 (1997).
[2] M. V. Wolkin, J. Jorne, P. M. Fauchet, G. Allan, and C. Delerue, Phys. Rev. Lett. **82**, 197 (1999).
[3] Y. Kanemitsu, H. Uto, and Y. Masumoto, Phys. Rev. B **48**, 2827 (1993).
[4] K. Koch and V. Petrova-Koch, in *Porous Silicon*, edited by Z. C. Feng and R. Tsu (World Scientific, Singapore, 1994).
[5] X. L. Wu, S. J. Xiong, D. L. Fan, Y. Gu, X. M. Bao, G. G. Siu, and M. Stokes, Phys. Rev. B **62**, R7759 (2000).
[6] F. S. Xue, X. M. Bao, and F. Yan, J. Appl. Phys. **81**, 3175 (1997).
[7] X. L. Wu and F. S. Xue, Appl. Phys. Lett. **84**, 2808 (2004).
[8] J. L. Gole, F. P. Dudel, D. Grantier, and D. A. Dixon, Phys. Rev. B **56**, 2137 (1997).
[9] S. M. Prokes, Appl. Phys. Lett. **62**, 3244 (1993).
[10] Y. H. Zhang, X. J. Li, L. Zheng, and Q. W. Chen, Phys. Rev. Lett. **81**, 1710 (1998).
[11] X. L. Wu, F. S. Xue, Z. Y. Zhang, G. G. Siu, and Paul K. Chu, Appl. Phys. Lett. **89**, 053114 (2006).
[12] M. C. Bost and J. E. Mahan, J. Appl. Phys. **58**, 2696 (1985).
[13] T. D. Hunt, K. J. Reeson, and R. M. Gwilliam, J. Lumin. **57**, 25 (1993).
[14] N. E. Christensen, Phys. Rev. B **42**, 7148 (1990).
[15] C. Giannini, S. Lagomarsino, and F. Scarinci, Phys. Rev. B **45**, 8822 (1992).
[16] H. W. Kroto, R. J. Heath, S. C. Brien, R. F. Caul, and R. E. Smalley, Nature (London) **318**, 165 (1985).
[17] B. Hamilton, J. S. Rimmer, M. Anderson, and D. Leigh, Adv. Mater. (Weinheim, Ger.) **5**, 583 (1992).
[18] L. Zhu and Y. Li, J. Appl. Phys. **77**, 2801 (1995).
[19] Y. H. Xie, W. L. Wilson, F. M. Ross, J. A. Mucha, E. A. Fitzgerald, J. M. Macaulay, and T. D. Harris, J. Appl. Phys. **71**, 2403 (1992).
[20] X. L. Wu, M. X. Liao, S. S. Deng, and G. G. Siu, J. Chem. Phys. **121**, 991 (2004).
[21] Z. Y. Zhang, X. L. Wu, T. Qiu, P. Chen, P. K. Chu, G. G. Siu, and D. L. Tang, J. Chem. Phys. **125**, 014706 (2006).
[22] X. L. Wu, G. G. Siu, M. J. Stokes, D. L. Fan, Y. Gu, and X. M. Bao, Appl. Phys. Lett. **77**, 1292 (2000).
[23] D. F. S. Petri, G. Wenz, P. Schunk, and T. Schimmel, Langmuir **15**, 4520 (1999).
[24] P. Zhou, A. M. Rao, K. A. Wang, J. D. Robertson, C. Eloi, M. S. Meier, S. L. Ren, X. X. Bi, P. C. Eklund, and M. S. Dresselhaus, Appl. Phys. Lett. **60**, 2871 (1992).
[25] X. L. Wu, F. Yan, X. M. Bao, S. Tong, G. G. Siu, S. S. Jiang, and D. Feng, Phys. Lett. A **225**, 170 (1997).
[26] G. D. Sanders and Y. C. Chang, Phys. Rev. B **45**, 9202 (1992).
[27] S. L. Chuang and C. S. Chang, Semicond. Sci. Technol. **12**, 252 (1997).
[28] M. Matus, H. Kuzmany, and E. Sohmen, Phys. Rev. Lett. **68**, 2822 (1992).